Online CD Performance Monitoring and Automatic Alignment Correction

Danlei Chu, Cristian Gheorghe, and Johan Backstrom

Honeywell Process Solutions, North Vancouver, BC, Canada V7J 3S4

ABSTRACT

Cross Directional (CD) alignment is a key component used in modeling and control of papermaking processes. It specifies the spatial relationship between the center of individual CD actuators and the center of the corresponding measurement responses. A poor CD alignment may cause the quality degradation of the finished product and unnecessary CD actuation at higher spatial frequencies which in turn can lead to higher production cost. This paper presents techniques for monitoring CD performance and correcting poor CD alignment in closed-loop. A revised accumulated sum algorithm is used to detect the onset of CD performance degradation and the pseudo random binary sequence (PRBS) is used in the identification of new CD alignment. The techniques presented in this paper have been implemented in industrial CD control systems and validated in multiple paper mills.

INTRODUCTION

Papermaking processes are large scaled two dimensional processes. They have to be monitored and controlled continuously in order to guarantee that paper quality is within the specifications of the finished product. There are two types of control problems involved in papermaking processes: cross directional (CD) control and machine directional (MD) control. Machine direction refers to the direction in which paper sheet travels and cross direction refers to the direction perpendicular to machine direction. The objectives of MD control and CD control are to minimize the variation of the sheet quality measurements in machine direction and cross direction, respectively. In general the CD control, either traditional Dahlin control [1], or multivariable model predictive control (MPC) [2], is model based. The good control performance is highly dependent on the accuracy of process models. CD alignment is a key model parameter that specifies the spatial relationship between the center of the individual CD actuators and the center of the corresponding measurement responses. It can change from time to time due to paper wander or shrinkage variation. A poor CD alignment may cause the degradation of the CD control performance and even the feedback instability. In practice a CD controller is tuned conservatively in order to tolerate the uncertainties of CD alignment. This is the robustness-performance tradeoff which is always encountered in a fixed parameter feedback controller. Automatic misalignment detection and closed-loop identification solution allow the CD controller to be tuned to provide a higher level of long term performance.

Fig. 1 illustrates the traditional way to identify the CD alignment model: the feedback CD controller is switched off and a set of CD individual actuators are displaced from the initial positions. Wait for a period of time until the process reaches the steady state. The experiment data including the actuator setpoints and the corresponding measurement responses are collected and transferred to a specialized software tool for alignment identification. This operation is called the open-loop bump test. A linear or nonlinear function is employed to map the coordinates of the center of the bumped actuators (a_1 to a_5 in Fig. 1) to the coordinates of the center of the corresponding responses (b_1 to b_5 in Fig. 1). The linear CD alignment model can be easily formulated by using the paper edges at the both actuator side and the measurement side. However, a nonlinear CD alignment requires additional parameters, not only the edge locations but also the web shrinkage profile. A fuzzy logic function presented in [3] specifies the characteristics of the typical non-uniform shrinkage profile across a paper web.

The open-loop bump tests are used widely in paper mills nowadays, but it has three obvious drawbacks: (1) the paper machine normal operation is interrupted; (2) it is time consuming; and (3) it requires the intervention of mill personnel. Different from the traditional bump tests, the adaptive alignment presented in this paper provides the closed-loop misalignment detection and the alignment identification algorithms. It monitors CD performance in closed-loop, perform the CD alignment identification if misalignment is detected, and updates the new alignment if the new alignment passes model validation and guarantees performance improvement after the deployment. The whole operation is fully automated and requires very litter or no user intervention. Both the linear CD alignment and nonlinear CD alignment are supported by the adaptive alignment.

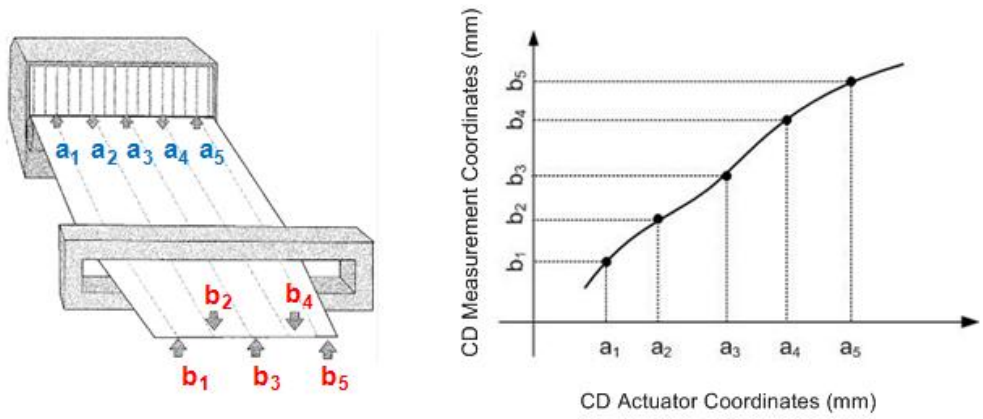

Figure 1: The Traditional Identification Approach for CD Alignment

OVERVIEW OF ADAPTIVE ALIGNMENT

The adaptive alignment has three major components: performance monitoring, closed-loop identification, and online deployment. Fig. 2 illustrates the design of each component.

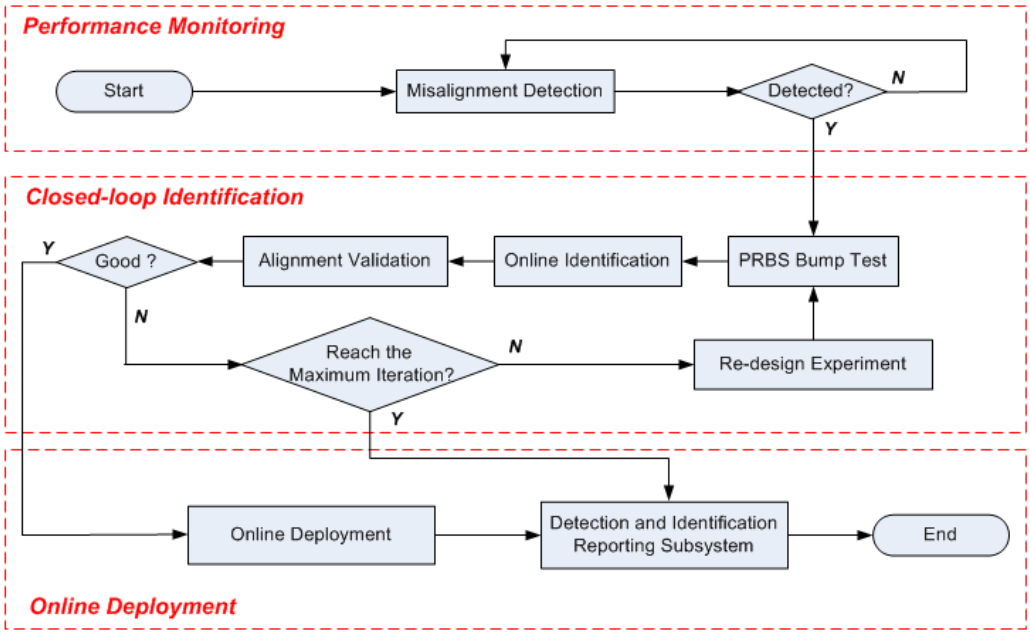

Figure 2: Overview of the Adaptive Alignment

The *misalignment detection* is the major function block of performance monitoring. It uses the quantification of actuator picketing as an indicator to trigger the closed-loop identification. Actuator picketing refers to a specific actuator setpoint profile pattern that looks similar to a picket fence. Fig. 3 shows the typical actuator picketing profile and the corresponding measurement profile observed on a production system which was operated under severe misalignment due to shrinkage changes. Both profiles are dominated by high spatial frequency components, and oscillate simultaneously under similar spatial frequencies. Actuator picketing has become a well-known symptom of CD misalignment and most paper mills rely on the operator's visual judgment to detect actuator picketing and request alignment identification. Different from the visual judgment approach, the detection algorithm presented in this paper takes advantage of the fact that actuator picketing causes the spatial power to increment in a certain high spatial frequency band for both actuator setpoint profiles and the CD measurement profiles. Once the

spatial power accumulation exceeds pre-specified thresholds, misalignment is said to be detected. Numerous mill trials have proven that the detection algorithm can detect the misalignment long before actuator picketing is visible to a paper machine operator. When using adaptive alignment, severe actuator picketing, as shown in Fig. 3, would have been effectively prevented.

In Fig. 2, *closed-loop identification* is triggered by performance monitoring. This means that the adaptive alignment starts identification experiments only if necessary. A Pseudo Random Binary Sequence (PRBS) is used to provide a low impact actuator excitation to the papermaking processes. Compared to traditional bump (step) tests, PRBS tests require shorter identification experiments, and also reduce the CD variability induced by the identification experiments. The PRBS design is intelligent and adapts to the process conditions. The magnitude, the location and the duration of the PRBS sequence are determined automatically based on the process' spatial and dynamic characteristics. The matrix inversion lemma [4] and stochastic signal processing techniques are used by the *online identification* function block in Fig. 2 to extract the open loop spatial response from the closed-loop experiment data. Refer to [5] for the details of theoretical analysis of the closed-loop identification algorithm. A reliable model validation algorithm is also provided by closed-loop identification component. The identified alignment is rated as either good or bad. If it is good, it will be deployed by *online deployment* component. Otherwise the adaptive alignment will start another PRBS test and try to re-identify the model. In the second PRBS test, slightly higher energy is injected into the process in order to improve the closed-loop identification.

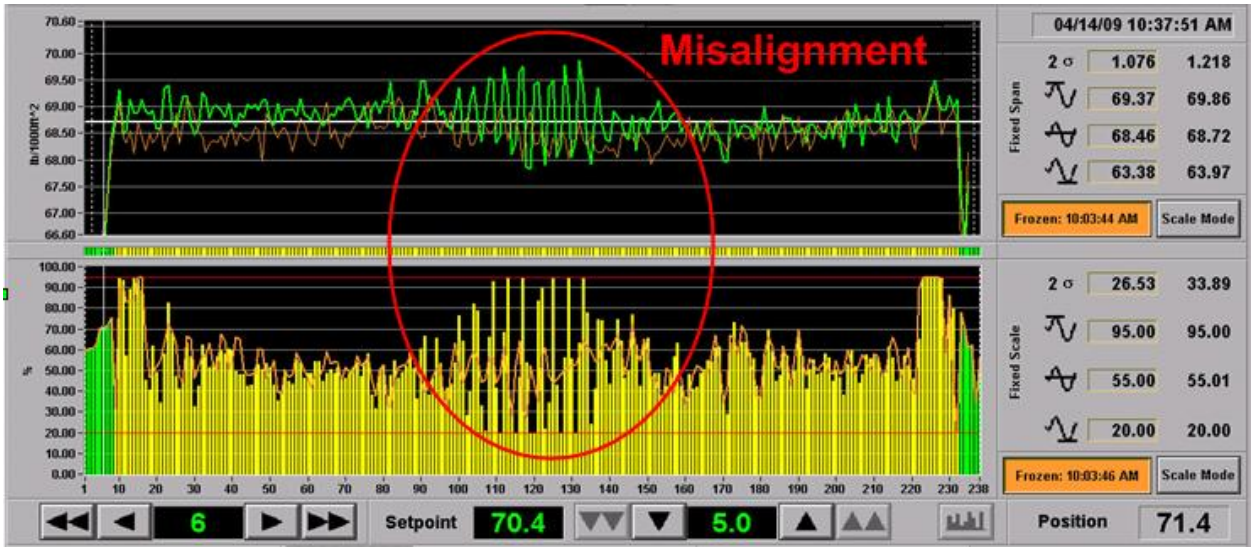

Figure 3: Actuator Picketing Profiles due to severe misalignment observed on a production system

The third component of Adaptive Alignment, called *Online Deployment*, is responsible for implementing the new CD alignment under closed loop CD control. It provides logic that guarantees that the overall closed loop performance is improved after deploying the new CD alignment. The *Detection and Identification Reporting Subsystem* block logs the key events of the adaptive alignment operation and provides a useful diagnosis tool in the case closed-loop identification does not provide reliable alignment information. It generates an analysis report for the possible causes of the identification failure, for example, the MD upsets are too large, signal-to-noise ratio is too small, or too many CD actuators under PRBS perturbation reach their physical constraints, etc. Similar to Misalignment Detection and Closed-loop Identification, *Online Deployment* is fully automated and no user intervention is required.

MISALIGNMENT DETECTION ALGORITHM

The key idea in Misalignment Detection is that the onset of actuator picketing results in the growth of the high frequency components in the actuator power spectrum. The detection algorithm performs a two-dimensional frequency analysis for both actuator setpoint profiles and quality measurement profiles. Fig. 4 illustrates this process.

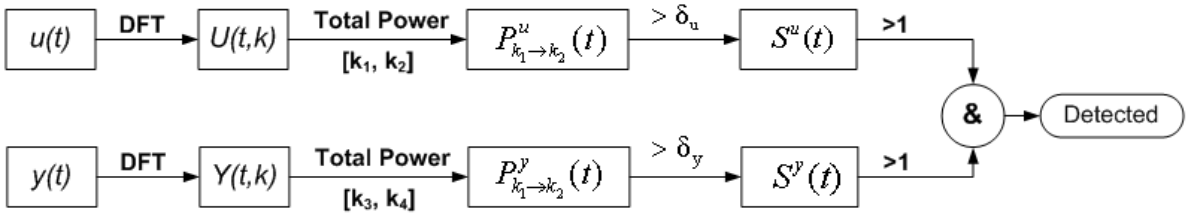

Figure 4: Performance Monitoring

Consider the actuator setpoint profile $u(t)$ and the measurement profile $y(t)$ at instant t. The power spectrums $U(t,k)$ and $Y(t,k)$ can be calculated by performing Discrete Fourier Transfer (DFT) on $u(t)$ and $y(t)$, respectively. The symbol k is the index of spatial frequencies. The power accumulations in the spatial frequency band $[k_1, k_2]$ for the actuator setpoint profile $u(t)$ and in the band $[k_3, k_4]$ for the measurement profile $y(t)$ can be calculated by,

$$P^u_{k_1\to k_2}(t) = \frac{1}{N}\sqrt{\sum_{k=k_1}^{k_2} U(t,k)\cdot conj(U(t,k))}, \tag{1}$$

and

$$P^y_{k_3\to k_4}(t) = \frac{1}{N}\sqrt{\sum_{k=k_3}^{k_4} Y(t,k)\cdot conj(Y(t,k))}. \tag{2}$$

where $P^u_{k_1\to k_2}(t)$ and $P^y_{k_3\to k_4}(t)$ are the power accumulation in the spatial frequency domain for the actuator and measurement profiles, respectively. *N* is the number of the DFT frequency points.

Based on $P^u_{k_1\to k_2}(t)$ and $P^y_{k_3\to k_4}(t)$, one can perform the power accumulation in the time domain, i.e., the two-dimensional power accumulations $S^u(t)$ and $S^y(t)$ for the actuator and measurement profiles are,

$$S^u(t) = S^u(t-1) + (\frac{P^u_{k_1\to k_2}(t-1)}{\delta_u} - 1), \tag{3}$$

and

$$S^y(t) = S^y(t-1) + (\frac{P^y_{k_3\to k_4}(t-1)}{\delta_y} - 1), \tag{4}$$

where $S^u(t) = 0$ if $t \le t_u$ and $S^y(t) = 0$ if $t \le t_y$.

t_u stands for the time tag when the actuator power accumulation starts in the time domain, i.e.,

$$P^u_{k_1\to k_2}(t_1) > \delta_u\,. \tag{5}$$

t_y indicates the time tag when the measurement power accumulation starts in the time domain, i.e.,

$$P^y_{k_3\to k_4}(t_1) > \delta_y\,. \tag{6}$$

Here δ_u and δ_y are the thresholds to trigger the power accumulation in the time domain for the actuator setpoints and the measurement profiles, respectively. Their values are determined by performing the CD performance baselining [5].

If the two dimensional power accumulations $S^u(t)$ and $S^y(t)$ are greater than 1 at instant t_{det}, misalignment is detected and the closed-identification is triggered. The reason the detection algorithm includes the measurement profiles $y(t)$ in the misalignment detection is to prevent false detection caused by overly aggressive CD tuning.

Fig. 5 shows the misalignment detection user display. *Spread Baseline* for the actuator setpoint profile is the threshold δ_u , currently set to 39.51; *Spread Baseline* for measurement profiles is the threshold δ_y, currently set to 0.98. These values are determined automatically by a one-button click (*Start Baselining* button). The baseline profiles are shown at the bottom of Fig. 5.

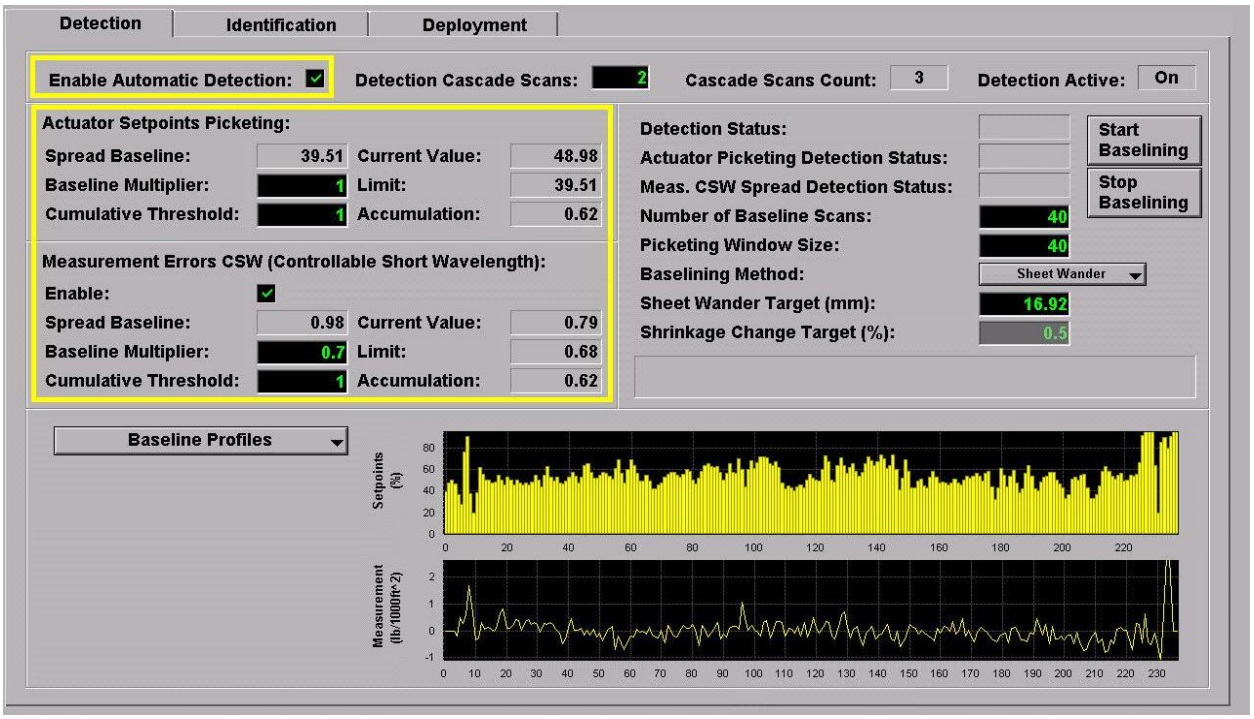

Figure 5: Misalignment Detection User Display

CLOSED-LOOP IDENTIFICATION ALGORITHM

A major technical challenge of closed-loop model identification is that the injected perturbation signal (dithering signal) is correlated with the output disturbances. Because of this correlation, methods that work well in the open loop may fail in the closed loop. The papermaking CD process is a large scaled two-dimensional process. It shows strong input-output off-diagonal coupling properties. The large dimension of the feedback CD processes makes the closed-loop CD identification even more challenging.

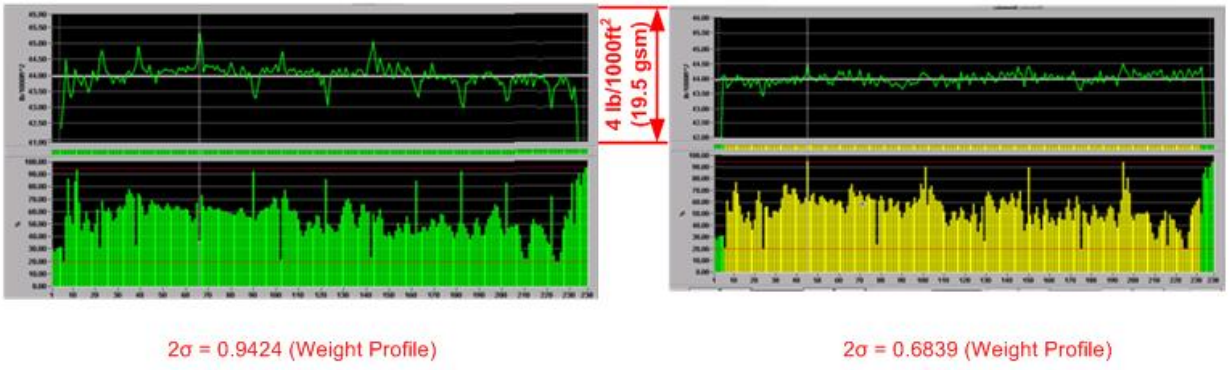

Figure 6: Comparison of the Open Loop Step Bump Test and the Closed Loop PRBS Bump Test

The closed-loop identification algorithm used by Adaptive Alignment has the feature to extract the open-loop spatial response from the closed-loop experiment data. PRBS tests are introduced to CD model identification. The

CD variance induced by PRBS tests is much smaller than the CD variance induced by persistent step bump tests. Fig. 6 shows the comparison between the open loop step bump test and the closed-loop PRBS bump tests. The induced 2σ (two times of the standard derivation of 238 measurement points) is reduced by 27.4% from 0.94 gsm (gram per square meter) to 0.68 gsm. In Fig. 6, the CD actuator is headbox dilution and the quality measurement is conditioned weight.

Let's assume the PRBS experiment data are $(v(t), y(t))$. $v(t)$ is the dithering signal and can be represented by

$$v(t) = U\phi(t). \tag{7}$$

Here $\phi(t)$ is a PRBS in the time domain and *U* is the constant spatial vector that defines the bumped individual actuator zones. From the definition of the PRBS, $\phi(t)$ satisfies

$$R_\phi(\tau) = \mathbf{E}\big(\phi(t)\phi(t-\tau)\big) = \begin{cases} R_\phi^0, & if\ \tau = 0 \\ 0, & if\ \tau \neq 0 \end{cases}. \tag{8}$$

where **E** is the expectation operator and $R_\phi(\tau)$ is the auto-covariance of $\phi(t)$. By performing the covariance analysis between the input and output, the open-loop spatial response, $\hat{g}_u$, can be extracted from the closed-loop experiment data $y(t)$,

$$\hat{g}_u = GU = \frac{R_{y\phi}(T_d+i)}{h_{T_d+i}R_\phi^0}\ (i = 0, \cdots, T_d - 1). \tag{9}$$

Here G is the spatial response matrix, T_d is the process time delay, and h_{T_d+i} is the coefficient of the finite impulse response (FIR) of the CD dynamic model.

After deriving the open-loop spatial response $\hat{g}_u$, the CD alignment identification is simplified to solve a nonlinear least square problem, i.e.,

$$\theta_M^0 = argmin_{\theta_M} ||g_u(\theta_M) - \hat{g}_u||_2^2, \tag{10}$$

where θ_M is the alignment parameter (either linear or nonlinear), and $g_u(\theta_M)$ is the open-loop response prediction based on θ_M. Refer to [3] for the details of the alignment parameter definition.

The closed-loop identification algorithm presented in this paper has following features:

- It is able to extract open-loop responses from the closed-loop experiment data. The CD feedback controller can attenuate the output disturbances during the identification experiments.
- The dithering signal $v(t)$ in Eq. (7) is two dimensional. The constant spatial vector *U* defines the individual actuators in the spatial domain, and the PRBS scalar sequence $\phi(t)$ defines the bump characteristics in the time domain. The design of PRBS is fully automated and it is able to adapt to the process situation.
- The algorithm can tolerate both spatial and dynamic model uncertainties, i.e., the uncertainties on G, T_d, and h_{T_d+i}.
- The algorithm supports both linear and nonlinear shrinkage identification.

Refer to [5] for the theoretical proof of the closed-loop CD identification algorithm in Eq. (9). Fig. 7 shows the closed-loop CD alignment identification user display. The profiles in the bottom graph are the predicted open-loop responses $g_u(\theta_M^o)$ (yellow line), and the identified open-loop responses $\hat{g}_u$ (green line). It can be clearly seen that the profiles of $g_u(\theta_M^o)$ and $\hat{g}_u$ have quite high fitness. This means that the identified alignment is closed to the real process alignment value. The quality of the identified alignment is quantified with a *Model Validation Qualifier*. Once the qualifier is *Good* it is safe to use the new alignment in the feedback CD controller. The model validation qualifier is used in the online alignment deployment logic, which guarantees that the CD control performance improves with the new alignement.

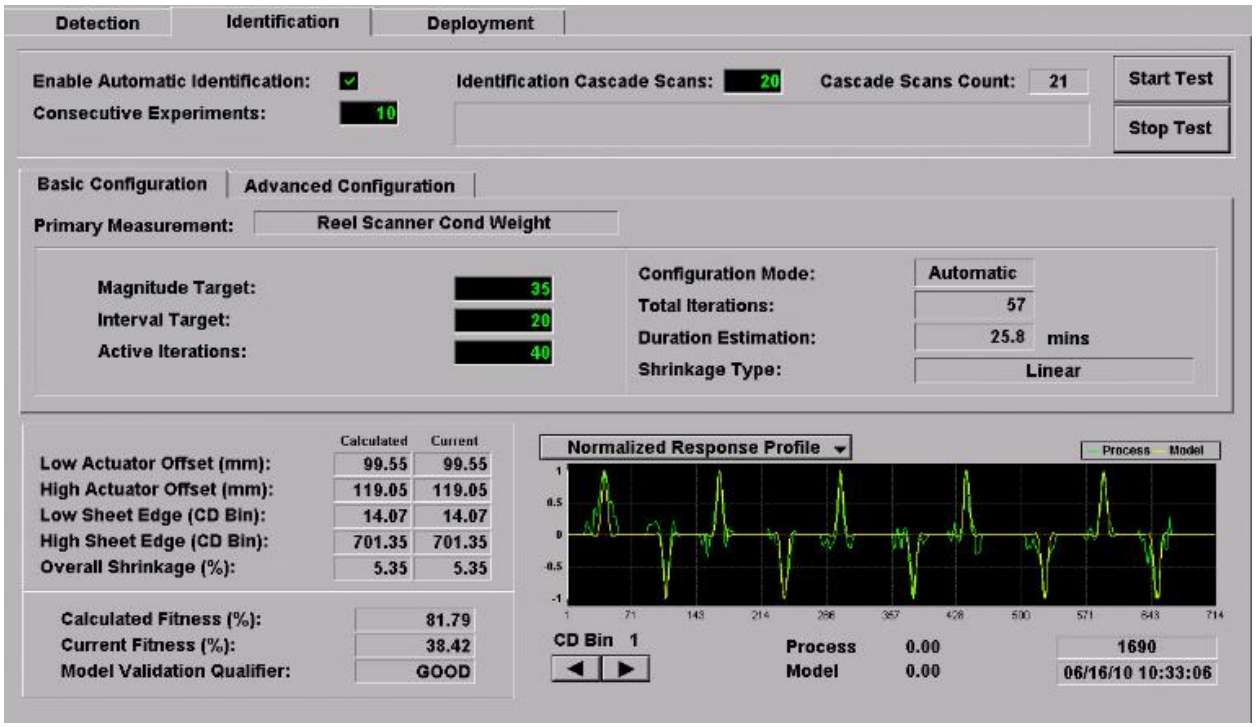

Figure 7: Closed-loop CD Alignment Identification User Display

MILL TRIAL RESULTS

The algorithm of adaptive alignment has been validated on different paper machines in North America. Trials to date under challenging process conditions have resulted in 18% - 24% reduction in product variability stemming from poor CD alignment. This section shows trial results from a wide linerboard machine to demonstrate the effectiveness of the detection and identification algorithms.

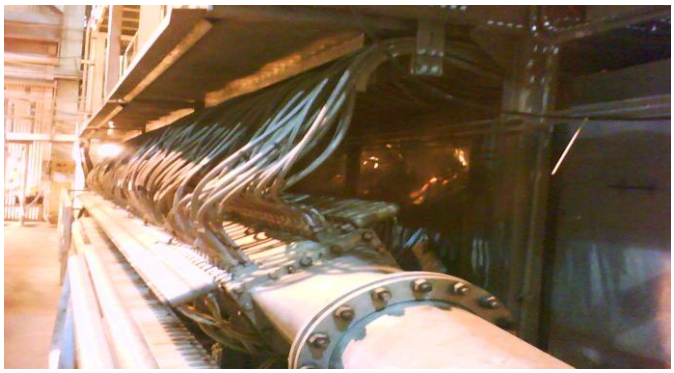

Figure 8: The Dilution Headbox

The linerboard machine has four CD actuator beams: headbox dilution, rewet shower, steambox, and induction heating, controlling three CD sheet properties: conditioned weight, moisture, and caliper (thickness). The feedback CD control is based on a multivariable distributed model predictive control strategy. The headbox dilution CD actuator beam (shown in Fig. 8) has relatively narrow actuator spacing, equal to 42 mm. It has a total 238 actuator zones evenly distributed across the paper machine. The narrow actuator spacing makes the CD controller sensitive to a poor CD alignment. Before the adaptive alignment was installed, the mill personnel had to regularly perform open-

loop bump tests and re-align the system. After the installation, misalignment is detected and corrected for automatically in closed-loop. There is very little or no user intervention.

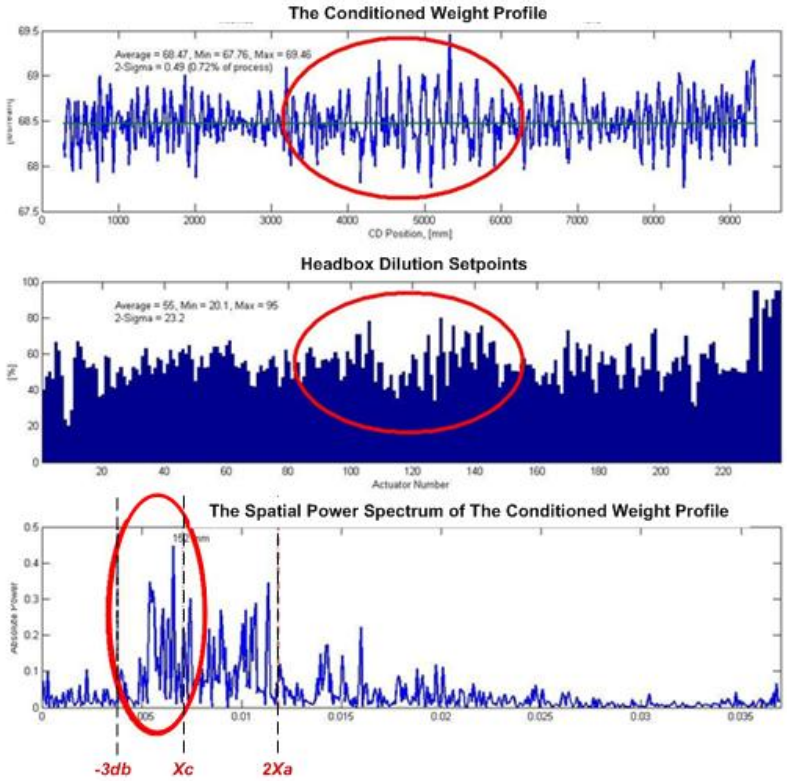

Figure 9: Actuator setpoints and measurement profiles before the closed-loop identification starts

The CD alignment of this machine can change from time to time typically due to shrinkage change or paper wander. The detection algorithm monitors the dilution actuator setpoints and the conditioned weight profiles in a continuous fashion. Fig. 9 shows the misalignment profiles just prior to triggering the closed-loop identification. The typical actuator picketing pattern can be vaguely observed in the center of the profiles, which indicates the occurrence of a very mild misalignment. The algorithm prevents the development of severe actuator picketing that has developed on this production system before the adaptive alignment installation (see Fig. 3). The bottom graph in Fig. 9 is the power spectrum of the conditioned weight profile. It can be seen that misalignment causes power accumulation between the spatial frequency $-3db$ and Xc. Here $-3db$ refers to the spatial frequency where the spatial process power drops to 50% of the maximum spatial power over the full spatial frequency band, Xc is the spatial frequency where the spatial process power drops to 4%, and $2Xa$ is the spatial Nyquist frequency.

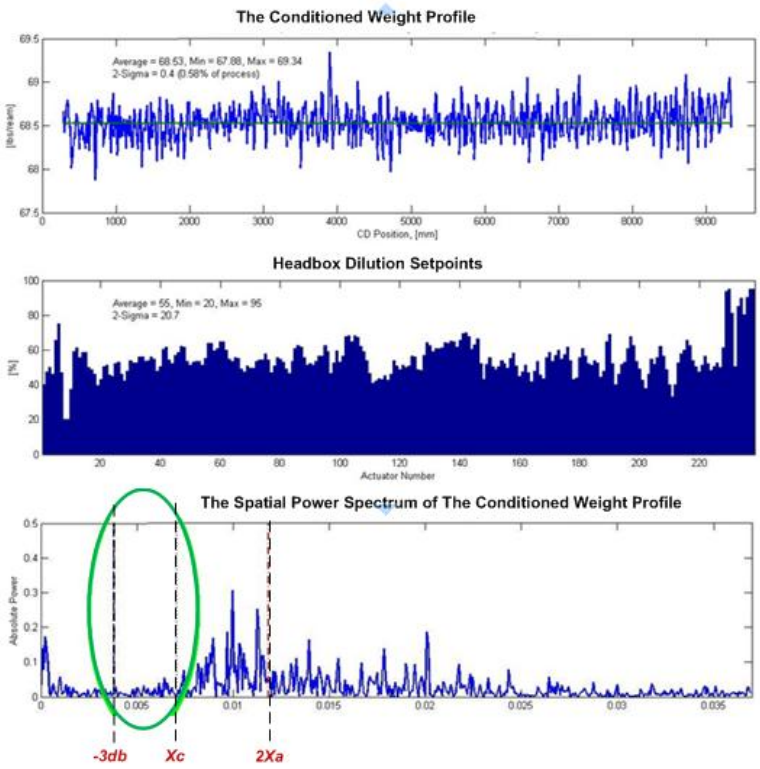

Figure 10: Actuator setpoint and measurement profiles after correcting the CD alignment

Fig. 10 shows the profiles after performing the closed-loop CD alignment identification and deploying the new CD alignment. The variability in the conditioned weight profile between the spatial frequencies $-3db$ and Xc have been attenuated effectively. The 2σ spread of conditioned weight (714 measurement points) dropped by 18.4% from 2.39 gsm to 1.95 gsm.

Fig. 11 shows the color maps of the logged profiles of dilution actuator setpoints and conditioned weight measurements during the adaptive alignment test. ***Region A*** between scans 1 - 120 represents the interval where the CD process was operated under misalignment. The barely noticeable diagonal streaks developed in the middle section of the sheet towards the end of region A. This snake skin pattern color map is a typical symptom of misalignment. ***Region B*** between scans 121 - 150 represents the interval where the actuator picketing and its generated diagonal streaks are gradually eliminated after the adaptive alignment has retuned the MPC controller automatically by using more conservative tuning parameters. The conservative tuning tolerates the alignment error and stabilizes the feedback CD controller. ***Region C*** between scans 151 - 190 shows the 10 actuators performing PRBS test for the closed-loop CD alignment identification. From the color map, one can see that the PRBS test has injected a set of irregular pulses into the process. These non-persistent pulses result in a very small amount of induced measurement variability compared to a conventional open loop step test. From the top color map, one can hardly see any increase in conditioned weight variance during the PRBS test. At completion (scan 190) the calculated alignment parameters are automatically deployed, along with restoring the original tuning. ***Region D*** starting at scan 191 shows that once the misalignment has been corrected, the CD controller provides high performance without the undesirable aspect of picketing that was initially present in region A.

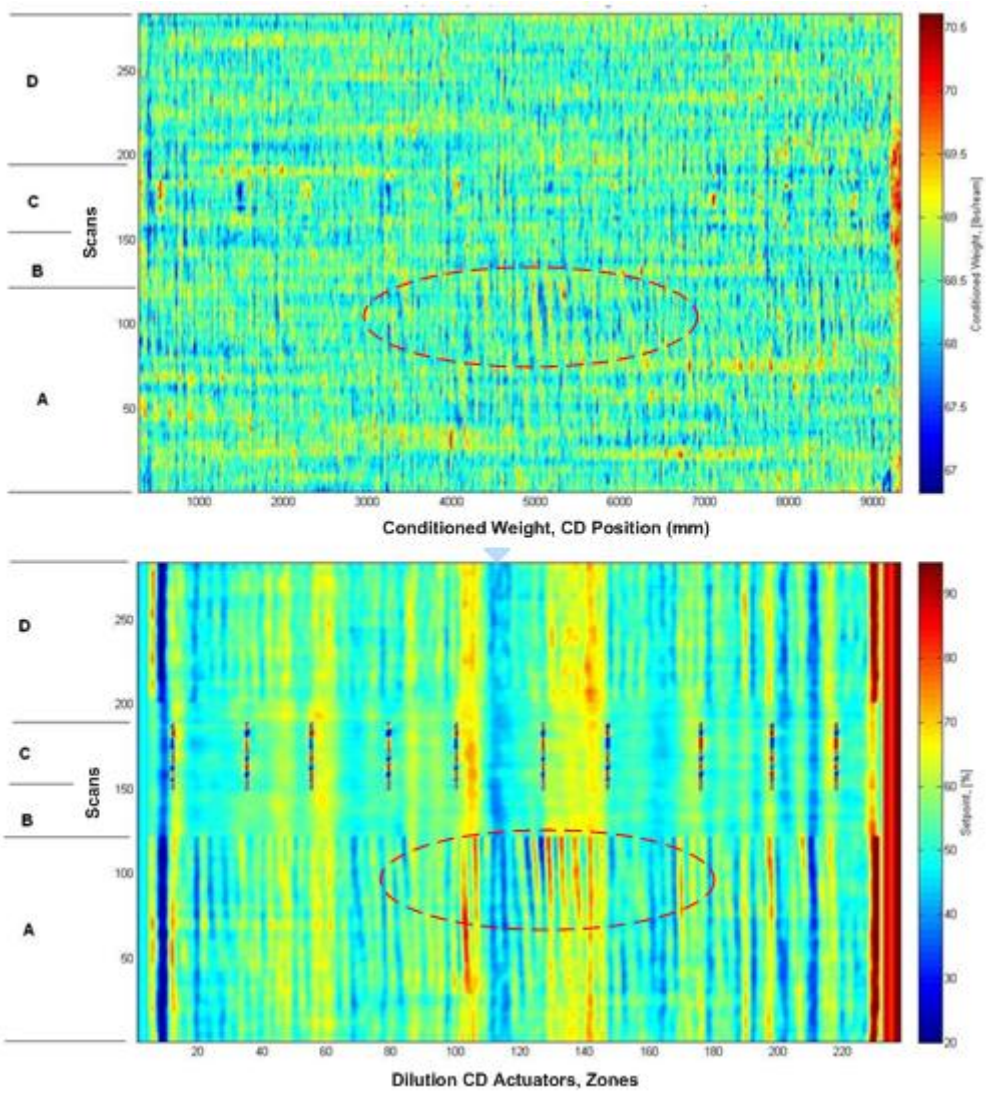

Figure 11: The color map of logged dilution actuator setpoint and conditioned weight profiles

CONCLUSION

This paper presents a closed-loop CD alignment solution. It is a true adaptive maintenance tool that is able to detect misalignment, run the identification, and deploy the new alignment in closed-loop. The whole process is fully automated. The adaptive alignment has been validated on different paper and board machines in North America and has shown to reduce product variability caused by CD misalignment by up to 24%.

REFERENCE

[1] E.B. Dahlin, "Design and Tuning Digital Controllers", in *Instrument & Control Systems*, Vol. 41, pp. 77-83, 1968.

[2] J. Backstrom, C. Gheorghe, G. Stewart, and R. Vyse, "Constrained model predictive control for cross directional multi-array processes", In *Pulp & Paper Canada*, May 2001, pp. T128– T102, 2001.

[3] D. Gorinevsky and C. Gheorghe , "Identification tool for cross-directional processes", in *IEEE Trans. on Control Systems Technology*, Vol. 11, pp. 629-640, 2003.

[4] K. Zhou and J. Doyle, *Essentials of Robust Control*, Prentice Hall, September 1997.

[5] D. Chu, J. Backstrom, C. Gheorghe, A. Lahouaoula, and C. Chung, "Intelligent Closed Loop CD Alignment", in *Proc. Control Systems 2010*, pp. 161-166, 2010.